

ANALYSIS OF PEDESTRIAN SHORT-TERM EXPOSURE ON A HIGH TRAFFIC CITY STREET

J. GARCIA¹, R. CERDEIRA¹, N. TAVARES¹, L.M.R. COELHO¹ & M.G. CARVALHO^{2,3}

¹Escola Superior de Tecnologia de Setúbal, Instituto Politécnico de Setúbal, Setúbal, Portugal.

²Instituto Superior Técnico, Portugal.

³Member of the European Parliament, Brussels, Belgium.

ABSTRACT

This article studies the influence of building street geometry, wind direction, daily car traffic and pedestrian trajectories in short-term personal exposure to PM_{10} on a street canyon in Barreiro City, Portugal. An automatic system for the analysis of traffic profiles, a Gaussian model for the determination of traffic emissions (ADMS-Urban) and a computational fluid dynamics model (ANSYS Fluent) to simulate the dispersion of pollutants inside a street canyon were used. Buildings height, width, length and geometry, as well as the distance between the buildings and road width were tested. Besides the real actual geometry of the street, with the real disposition and volumetric configuration of buildings, three scenarios were evaluated: (i) gaps of 4 m between the buildings along the street; (ii) gaps of 6 m between the buildings along the street and (iii) same height and width for all buildings along the street without gap between buildings. Wind direction, wind velocity and four pedestrian trajectories were considered. The results show that PM_{10} concentration, at 1.5-m high plane, is highly dependent on street geometry and wind conditions for along-canyon wind directions (west and east wind). Lower concentration levels are obtained for configuration (iii) because this geometry promotes the dispersion of pollutants under along-canyon wind direction. For cross-canyon wind directions (north and south), configuration (i) results in lower PM_{10} concentrations. There are no visible improvements in having higher gaps between buildings (configuration ii). Short-term pedestrian personal exposure is dependent on the pedestrian trajectory considered inside the canyon. Pedestrian trajectories that correspond to crossing the road in the centre of the street result in the highest values.

Keywords: Air quality, PM_{10} , short-term personal exposure, street canyon, urban planning.

1 INTRODUCTION

One of most important items on public health in cities is the Urban Air Quality levels. In this matter, particle concentration in streets is one major issue. Topography and urban obstructions such as buildings have great influence on the atmospheric flow and consequently on the pollutants dispersion. This effect change the pollutant dispersion, particularly vehicle exhaust pollutants, which cannot be carried away by the wind, due to buildings that act as barriers, avoiding the wind circulation. Dispersion cannot occur since air and consequently air pollutants are trapped within the street canyon, raising the concentration of this contaminant. Therefore, for decision makers, it is important to know what is the influence of building volume and geometry on air quality in a street. Computational fluid dynamics (CFD) models have been highly developed and are now a very reliable tool for simulating pollutant concentrations in urban areas. Very satisfactory modeling accuracy is now possible, mainly due to the continuous important development of very powerful numerical codes, parallel to fantastic increases in hardware performances. Complementary with this computational tools, measurement campaigns are also very important, because they contribute to validate the simulations and help in understanding the accuracy of computational results. In the range of air pollutants, particular attention was dedicated to particulate matter (PM) considering both PM_{10} and $PM_{2.5}$ [1,2] and more recently nanoparticle [3]. Most epidemiological studies have focused on PM_{10} and $PM_{2.5}$, and there is certain evidence that short-term exposure to high concentrations of PM_{10} can aggravate pulmonary diseases and have influence on paediatric

asthma [4], and long-term exposure to high concentrations on PM_{10} may increase the risk of cardiovascular disease and pulmonary disease. This article studies the influence of personal exposure to PM_{10} on a particular street in Barreiro city, in Portugal considering particularly different pedestrian ways in that street.

2 THE STUDIED STREET

Avenida do Bocage is a street located in Barreiro city in Portugal. Barreiro is a medium size city located 40 km south of Lisbon, Portugal (Fig. 1). This is a small city, over 34 km² and 80,000 inhabitants, with industry near the centre and typical city traffic. Barreiro is almost flat, with the highest point at approximately 10 m above the sea level. The weather is temperate, with no severe seasons. Avenida do Bocage is an important strategic key point in the city, because it connects the city centre with an important highway from the capital of Portugal, Lisbon. Therefore, the traffic flux is very important especially in rough hours, representing the main source of pollution in the street. The importance of this street is also connected with the fact that it has inside a primary school and with the fact that represent an important pedestrian way to people who go to the river or to the fluvial station. A part of this street is the domain considered in this study.

3 SHORT CHARACTERIZATION OF POLLUTANT SOURCES

The main industrial activity in Barreiro city is developed in the industrial area, near the city centre. A natural gas power plant and some chemical industries are the main industrial sources. The most important pollutants released from this source are NO_x , SO_2 and PM. These pollutant concentrations are continuously monitored. Traffic is the major pollutant source, like in other cities, due to the continuous population growth in urban areas and lack of efficient public transports. Light duty vehicles (LDV) constitute the most important traffic fraction, however, and due to the proximity of the industrial area, heavy duty vehicles (HDV) have an important contribution in pollutants concentration. A traffic characterization was carried out in Barreiro city streets, considering the number of vehicles per type, used fuel, velocity, street characteristics and the time of the day when the field campaign was made. Other sources, such as residual, poorly-defined or diffuse emissions in urban areas, like minor roads, were also considered, as well as the background pollutant concentrations.

4 METEOROLOGICAL CHARACTERIZATION OF THE CITY

The identification of the main meteorological parameters of Barreiro city was made on the basis of meteorological weather station Lavradio, from Instituto de Meteorologia (IM), which is the closest to the study area. The prevailing wind direction is NW (frequency 35.1%). The highest wind speeds

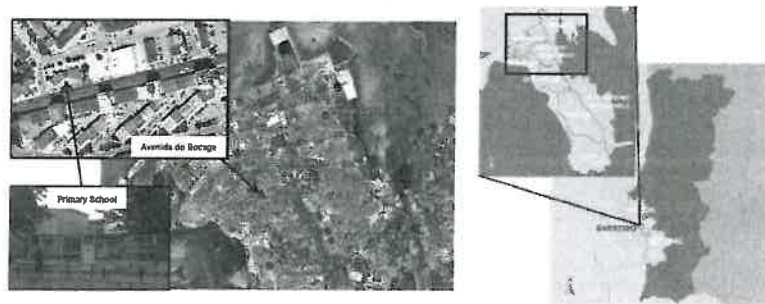


Figure 1: Location of Avenida do Bocage in Barreiro, Portugal.

registered correspond to the South direction (15.2km/h) seconded by the prevailing direction NW (14.1 km/h). The NW wind is particularly frequent in the summer months (June, July and August), the maximum occurring in August (58.5%). The minimum frequency of values was recorded in December (15.6%). The average wind speed is relatively constant throughout the year. Concerning the atmosphere stability, it was not possible to calculate the stability classes to Barreiro due to the lack of cloudiness and radiation data required by the model. For this reason, Setúbal city stability classes were used, since atmospheric conditions at both cities are similar, as well as their location. The frequency of occurrence of each stability class is presented in Table 1 for Setúbal, being neutral stability class the most frequent one.

5 THE INTEGRATED SYSTEM

For the development of this study, an integrated system was build considering atmospheric wind profile resulting from weather conditions, street geometry and emissions from urban traffic in the avenue. Figure 2 shows the integrated global system structure, considering all sub-models and the traffic counting system. The study domain is initially drawn in the computer program Autocad, where Bocage Avenue is represented three-dimensionally, with their buildings. This 3D design is subsequently exported to

Table 1: Frequency of occurrence of stability classes for Setubal [5].

| Stability class | Frequency (%) |
|-------------------|---------------|
| Very unstable | 0.24 |
| Unstable | 16.00 |
| Slightly unstable | 20.31 |
| Neutral | 46.90 |
| Slightly stable | 3.25 |
| Stable | 6.82 |
| Very stable | 6.48 |

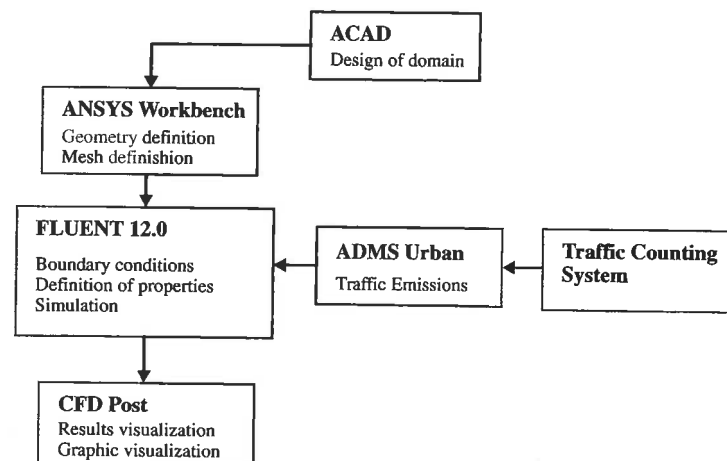


Figure 2: The architecture of the developed integrated system.

ANSYS Fluent Workbench [6], where the boundaries are defined, as well as the mesh. These data are exported to Fluent where the mesh is verified, and all properties are set, as well as the physical models. Fluent receives data from traffic emissions calculations made by ADMS Urban sub-model [7]. The traffic emission calculated by ADMS is based on the results received from the traffic counting system, especially designed for this application. In Fluent, the convergence criteria are defined, the solution is initialized and the calculations are performed. After having achieved convergence calculations, all results are transferred to the CFD Post (post-processor) where the results are displayed.

6 THE TRAFFIC COUNTING SYSTEM

Road traffic is the major source of pollutants in the street. For the proper characterization of particulate emissions in the Bocage Avenue, a traffic counting system was designed, developed and implemented. This system counts vehicles moving along the road; it is also possible to identify the type of vehicle (light or heavy duty) and it allows calculating the running speed, in order to make a characterization as accurate as possible of PM emission. The system consists of two photocells long distance retro-reflective from Omron, Model E3G-L73 2M, a PLC (programmable controller) also from Omron, CP1L, a laptop from HP and software programming. The system architecture is depicted in Fig. 3, the working principle is shown in Fig. 4. and in Fig. 5 it is possible to see a picture of the road traffic counting system implemented in the street.

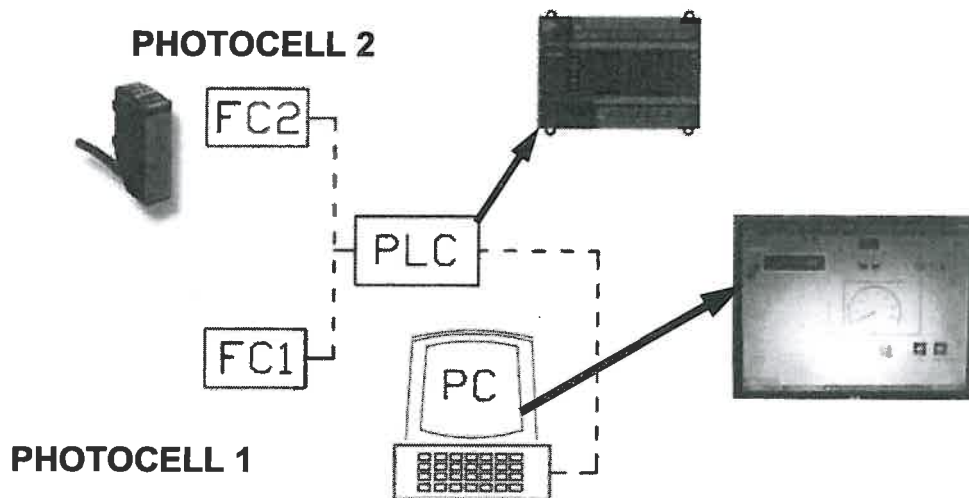


Figure 3: The architecture of the system developed for road traffic count.

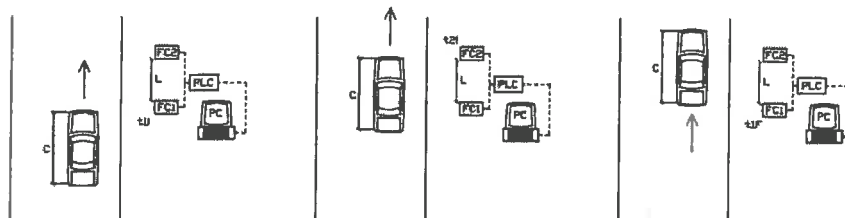


Figure 4: The working principle of the system developed for road traffic count.

The counting in the road was divided into three periods: 8–10, 12–13 and 17–20 h dated 21/07/2010 to 23/07/2010. The vehicles counting was made for 1 h in each period. The vehicles were classified according to the class (light and heavy duty, heavy passenger and motorcycles). The main characteristics of the road, as the width, the average height of the buildings and the type of the road (in this case urban) were also considered. The values for PM_{10} emission from car traffic were then calculated by ADMS-Urban model.

7 THE CFD MODEL

For the study of the dispersion of PM_{10} on the street, a CFD simulation was carried out. ANSYS Fluent 12.0 software was used; this software is a multi-purpose commercial software, widely used in this kind of application and constantly validated through comparison of results with other validated models [8] or through wind tunnel experiences [9]. To fulfil the aim of this study, a spatial discretization of the computational domain was made. A tetrahedral grid was used, refined near the buildings. The geometry of the street is shown in Fig. 1. As different wind directions were studied, different domains were used to assure sufficient distance between the buildings and the domain boundaries in the simulation. A 3D flow simulation with a Lagrangian approach was used, assuming steady-state conditions, and for the turbulence, the κ - ϵ turbulence model was used, more precisely the RNG κ - ϵ turbulence model. This model provides an analytical formula for turbulent Prandtl numbers and an analytically derived differential formula for effective viscosity that accounts for low-Reynolds-number effects [10]. A wind profile, turbulent kinetic energy and turbulence dissipation rate were introduced as a user-defined function (UDF) considering a log-law vertical wind profile. The two-way street PM_{10} car emission rate was introduced, using the ADMS-Urban model, and considering the traffic that crosses the street. No chemical reactions were considered for PM_{10} emissions. In terms of boundary conditions, a no-slip condition was imposed at all solid surfaces (the flow in the near-wall region was represented by the law-of-the-wall for mean velocity), whereas at the top a symmetry boundary was considered, assuming a zero flux for all quantities across the horizontal plane. For this study and considering west wind direction, the simulation domain considered was a $715 \times 300 \text{ m}^2$ centred in the Av Bocage with approximately 1,60,200 cells.

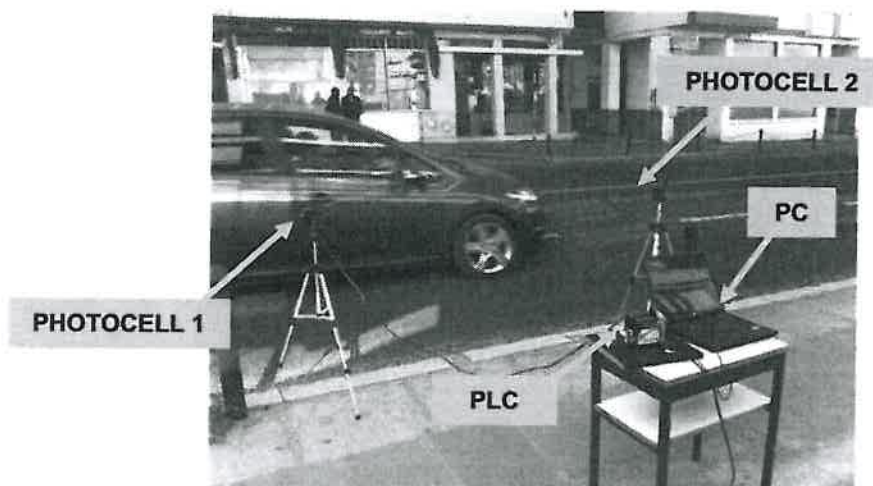


Figure 5: The road traffic counting system implemented in the street.

PM_{10} emissions were calculated by the model ADMS Urban, considering the traffic counting described in the early section. The emissions were introduced in Fluent as line sources and considering the mean traffic number of vehicles in rush hours as the baseline scenario for traffic emissions. The other emissions considered in the domain were introduced as background concentrations and summed to Fluent results. The value for background concentrations was collected from the Fidalguinhos Air Quality Station from the Portuguese AQ system, as this station is classified as urban background station. The model validation was made using real measurements of PM_{10} concentrations made in the street [11].

8 THE STREET CONFIGURATION SCENARIOS

The domain of this study (a part of Avenida do Bocage) is a configuration of continuous irregular buildings in one side of the street and some non-continuous buildings on the other side of the street. In this study, four scenarios of different configurations of Avenida do Bocage were considered, concerning building disposition. The first scenario corresponds to the actual street geometry, with the real architectural layout, disposition and volumetric configuration of buildings (Disposition A). Three other virtual dispositions for the street buildings were simulated, considering the alteration of buildings configurations, with the objective of trying to improve the air quality in this street. The first new virtual configuration, designed as Disposition B, considers the introduction of 4-m gaps between buildings along the street. The scenario designed as Disposition C was also tried, considering gaps of 6 m between buildings along the street. Finally, the scenario designed as Disposition D considers the same volume as actual real disposition for the buildings along the street, but with the same height and width for all buildings without gaps between them. The four building disposition scenarios are shown in Fig. 6.

9 RESULTS

The results for PM_{10} concentrations in the street were obtained with ANSYS Fluent 12.0. Figure 7 shows the concentration results obtained for PM_{10} simulations for horizontal concentrations fields to Disposition A, considering the four wind directions. Contours of PM_{10} concentrations at 1.5-m high

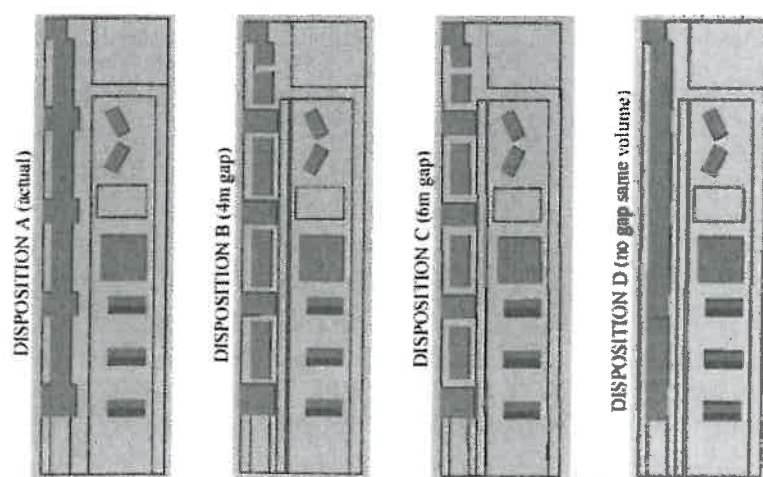


Figure 6: The four street disposition scenarios considered.

(considered the medium typical human nose level and used in frequent exposure studies) considering only traffic emissions (no background concentrations) are shown.

In Table 2, the values of PM_{10} simulated concentrations at 1.5-m high considering all the emissions (traffic + background) for Disposition A configuration are shown. These concentrations are shown for seven strategic points located in the street. Additionally, the mean concentration value for a plane located 1.5-m high and also the mean concentration at 1.5-m high weighted by the wind frequency

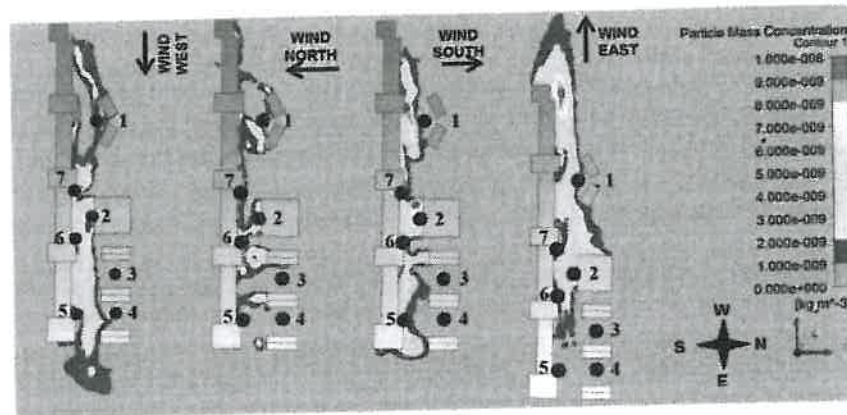


Figure 7: Contour plots of PM_{10} concentrations at 1.5-m level for the actual street configuration (Disposition A) for the main four wind directions.

Table 2: PM_{10} concentrations at 1.5-m high for disposition A (actual real configuration).

| Designation | Location | PM_{10} conc. ($\mu g/m^3$) | | | | CW ($\mu g/m^3$) |
|-------------|-----------------------------|---------------------------------|------------|------------|-----------|--------------------|
| | | West wind | North wind | South wind | East wind | |
| Point 1 | School | 21.6 | 21.2 | 20.7 | 22.3 | 21.3 |
| Point 2 | Bingo | 23.0 | 28.6 | 27.1 | 27.0 | 25.4 |
| Point 3 | Car park (border) | 20.1 | 20.0 | 20.1 | 20.0 | 20.1 |
| Point 4 | Car park (middle) | 20.4 | 20.0 | 20.1 | 20.0 | 20.2 |
| Point 5 | High building corner | 20.5 | 20.6 | 22.7 | 20.0 | 20.9 |
| Point 6 | Residential building (east) | 22.2 | 21.5 | 21.9 | 21.0 | 21.7 |
| Point 7 | Residential building (west) | 25.0 | 20.9 | 22.5 | 20.7 | 22.8 |
| Mean value | 1.5-m plane (all domains) | 20.8 | 20.5 | 21.0 | 21.1 | — |

are shown, this value is designed by CW (weighted concentration). The CW is estimated using eqn (1), which is the mean concentration weighted by the wind direction frequency (f_i), i.e. the average number of times in each year each direction was observed. This allows evaluating particles concentration for 1 year considering all actual different wind directions.

$$CW = C PM_{10} \times f_i \quad (1)$$

where $C PM_{10}$ is the concentration of PM_{10} ($\mu g/m^3$) and f_i is the wind direction frequency.

The simulation results show that the highest value of PM_{10} concentration is achieved in point 2 (Bingo building) with a value of $28.6 \mu g/m^3$ for North wind conditions. This point is located on the north end of the road near the largest building on this side, making difficult for the upstream wind to carry the pollutant outside the street. This point also corresponds to the highest value considering the CW, but if we consider the mean value of concentrations at 1.5-m high plane for the entire domain, the highest value is achieved for east wind conditions with a mean value of $21.1 \mu g/m^3$.

Results obtained for the simulations with the new configurations are shown in Figs. 8–10 (traffic) and in Tables 3–5 (background + traffic). Figure 8 shows the results obtained for the simulations for

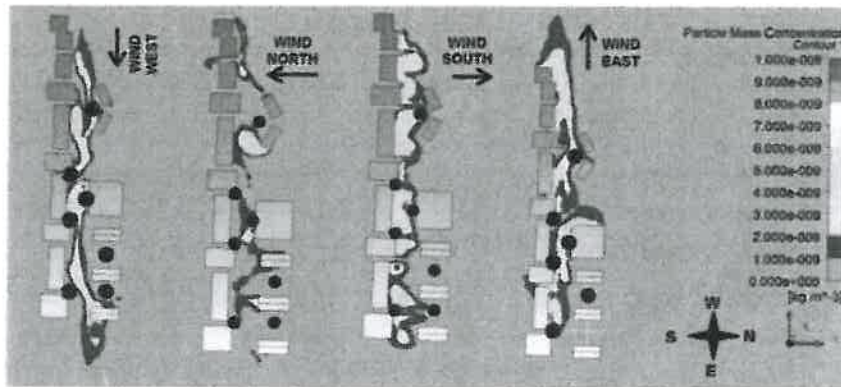


Figure 8: Contour plots of PM_{10} concentrations at 1.5-m level for Disposition B (4-m gap) for the main four wind directions.

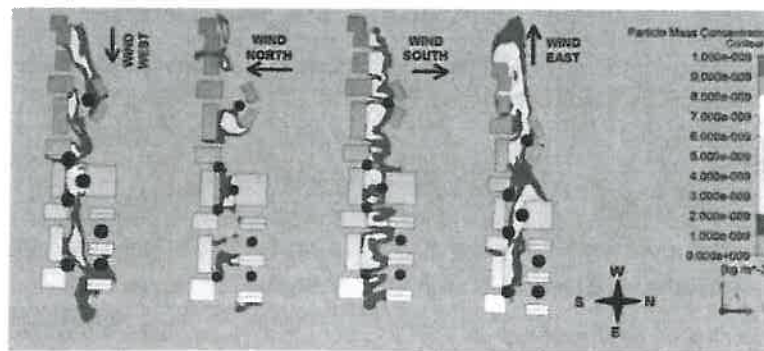


Figure 9: Contour plots of PM_{10} concentrations at 1.5-m level for Disposition C (6-m gap) for the main four wind directions.

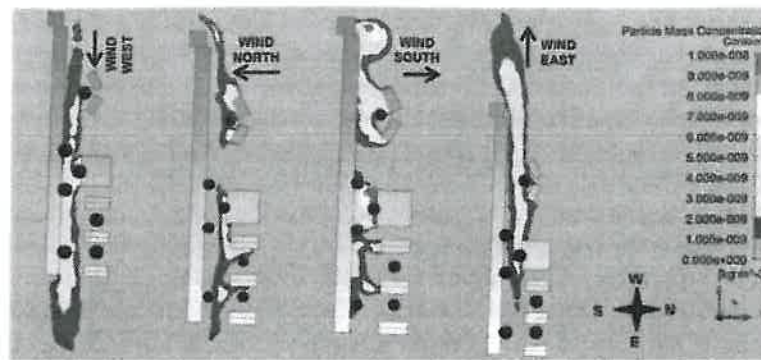


Figure 10: Contour plots of PM_{10} concentrations at 1.5-m level for Disposition D (no gap and same volume) for the main four wind directions.

Table 3: PM_{10} concentrations at 1.5-m high for disposition B (4-m gap).

| Designation | Location | PM_{10} Conc. ($\mu g/m^3$) | | | | CW ($\mu g/m^3$) |
|-------------|-----------------------------|---------------------------------|------------|------------|-----------|-----------------------|
| | | West wind | North wind | South wind | East wind | |
| Point 1 | School | 22.3 | 20.8 | 22.7 | 22.2 | 21.8 |
| Point 2 | Bingo | 25.7 | 23.2 | 21.8 | 27.6 | 24.1 |
| Point 3 | Car park(border) | 20.0 | 20.0 | 20.0 | 20.0 | 20.0 |
| Point 4 | Car park (middle) | 20.0 | 20.0 | 20.7 | 20.0 | 20.1 |
| Point 5 | High building corner | 20.0 | 20.0 | 20.4 | 21.2 | 20.2 |
| Point 6 | Residential building (east) | 21.0 | 20.1 | 23.9 | 20.7 | 21.2 |
| Point 7 | Resid. building (west) | 23.3 | 20.0 | 21.2 | 20.0 | 21.6 |
| Mean value | 1.5-m plane (all domains) | 20.5 | 20.3 | 20.6 | 20.8 | — |

Table 4: PM_{10} concentrations at 1.5-m high for disposition C (6-m gap).

| Designation | Location | PM_{10} conc. ($\mu g/m^3$) | | | | CW ($\mu g/m^3$) |
|-------------|-----------------------------|---------------------------------|------------|------------|-----------|-----------------------|
| | | West wind | North wind | South wind | East wind | |
| Point 1 | School | 20.9 | 20.8 | 21.0 | 21.2 | 20.8 |
| Point 2 | Bingo | 25.9 | 26.8 | 21.1 | 26.8 | 24.9 |
| Point 3 | Car park(border) | 20.0 | 20.0 | 20.3 | 20.0 | 20.1 |
| Point 4 | Car park (middle) | 20.4 | 20.0 | 20.5 | 20.0 | 20.3 |
| Point 5 | High building corner | 20.0 | 20.0 | 20.1 | 20.1 | 20.1 |
| Point 6 | Residential building (east) | 20.1 | 20.1 | 20.2 | 20.5 | 21.2 |
| Point 7 | Resid. building (west) | 22.9 | 22.9 | 20.0 | 20.1 | 21.2 |
| Mean value | 1.5-m plane (all domains) | 20.6 | 20.6 | 20.6 | 20.9 | — |

Table 5: PM₁₀ concentrations at 1.5-m high for disposition D (no gap, same volume).

| Designation | Location | PM ₁₀ conc. (µg/m ³) | | | | CW (µg/m ³) |
|-------------|-----------------------------|---|------------|------------|-----------|----------------------------|
| | | West wind | North wind | South wind | East wind | |
| Point 1 | School | 20.0 | 21.3 | 21.5 | 22.0 | 20.8 |
| Point 2 | Bingo | 24.1 | 22.8 | 30.7 | 23.0 | 24.7 |
| Point 3 | Car park(border) | 20.0 | 20.1 | 20.0 | 20.0 | 20.0 |
| Point 4 | Car park (middle) | 20.0 | 20.2 | 20.6 | 20.0 | 20.0 |
| Point 5 | High building corner | 23.2 | 20.4 | 21.1 | 20.1 | 21.6 |
| Point 6 | Residential building (east) | 23.3 | 20.0 | 21.9 | 20.4 | 21.8 |
| Point 7 | Resid. building (west) | 22.2 | 22.2 | 21.4 | 20.7 | 21.3 |
| Mean value | 1.5-m plane (all domains) | 20.3 | 20.4 | 20.8 | 20.6 | — |

PM₁₀ concentrations horizontal fields for Disposition B (traffic only). Figure 9 shows the results obtained for the simulations for PM₁₀ concentrations horizontal fields for Disposition C (traffic only). Figure 10 shows the results obtained for the simulations for PM₁₀ concentration horizontal fields for Disposition D (traffic only). In these figures, contours of PM₁₀ concentrations at 1.5-m high, considering only traffic emissions (no background concentrations), are shown for the four main wind directions studied. Tables 3–5 show the values of PM₁₀ simulated concentrations at 1.5-m high considering all the emissions (traffic + background) for the four scenarios considered, dispositions A, B, C and D.

By the analysis of Fig. 8 and Table 3, it is visible that the implementation of a 4-m gap between buildings decreases the concentrations of PM₁₀ in the street, considering the cross-canyon wind directions. This is due to the fact that these gaps between buildings reduce the effects of vortex creation in the street since there is no barrier to the wind, resulting in a better capacity of pollutants dispersion along the street, decreasing the PM₁₀ concentrations.

The results of Fig. 9 (traffic) and Table 4 (background+traffic) show that with the implementation of a 6-m gap between buildings (disposition C) compared with the scenario of having 4-m gap between buildings (disposition B) does not represent a visible decrease in PM₁₀ concentrations along the street, concluding that increasing the gap length does not bring significant improvements in the street air quality.

The results of Fig. 10 and Table 5 show that the solution of considering buildings with no gap but with the same volume represents a good option, promoting good pollutant dispersion, especially for along-canyon wind directions.

10 SHORT-TERM PEDESTRIAN PERSONAL EXPOSURE RESULTS

Four pedestrian trajectories were considered for people walking along the street in the direction of the fluvial station, with the objective of studying the influence of the four different scenarios (A, B, C and D) in short-term personal exposure to PM₁₀. The four pedestrian trajectories are shown in Fig. 11 and the characterization is made in Table 6.

Short-term personal exposure $E(t)$ in a period of time t can be expressed as [12]

$$E(\Delta t) = \int_0^t C(t) dt \equiv \sum_i C_i t_i \quad (2)$$

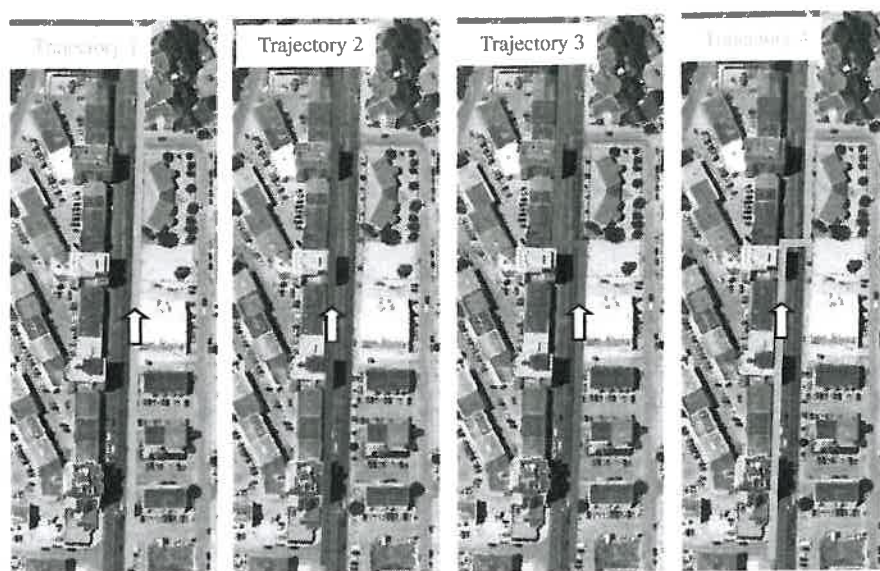


Figure 11: The four pedestrian trajectories considered.

Table 6: Short resume of the four pedestrian trajectories.

| Pedestrian trajectory | Description of trajectory | Total walking distance (m) | Walking mean velocity (m/s) | Total time (s) |
|-----------------------|---------------------------|----------------------------|-----------------------------|----------------|
| 1 | Only north side | 300 | 1.0 | 300 |
| 2 | Only south side | 300 | 1.0 | 300 |
| 3 | North to south | 310 | 1.0 | 310 |
| 4 | South to north | 310 | 1.0 | 310 |

where $C(t)$ is the pollutant concentration in a specific time t in $\mu\text{g}/\text{m}^3$, C_i is the discrete concentration in cellule i in $\mu\text{g}/\text{m}^3$ and t_i is the time of exposure in cellule i in seconds.

To calculate the total exposure related with each of the pedestrian trajectories, the computational domain was discretized in a grid with 240 cellules and 279 nodes, each one corresponds to 10 s time walk trajectory. The short-term personal exposure (E) was calculated in the nodes corresponding to the four pedestrian trajectories considered. This discrete grid is shown in Fig. 12.

The results obtained for this short-time personal exposure to PM_{10} , in $\mu\text{g h}/\text{m}^3$, for the four scenarios (A, B, C and D) under the four main wind directions and to the four pedestrian trajectories considered (1, 2, 3 and 4) are shown in Table 7.

It is possible to verify that in a global way Scenario A is the worst street configuration concerning short-term personal exposure, and Scenario C is the best configuration concerning short-term personal exposure, but the results are very similar to the ones obtained with Scenarios B and D. The highest values for short-term personal exposure are obtained for pedestrian trajectories 3 and 4 for Scenario A, under East wind conditions. It is visible that pedestrian trajectories 3 and 4 are always

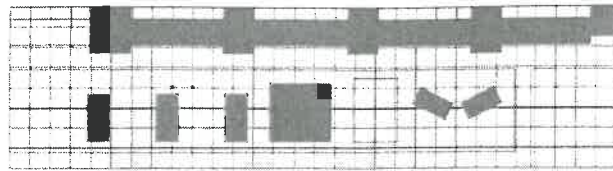


Figure 12: The discrete grid used in short-time exposure calculations.

Table 7: Short-term personal exposure to PM_{10} for the four trajectories considered (values in $\mu g\ h/m^3$).

| | Scenario A | | | | Scenario B | | | | Scenario C | | | | Scenario D | | | |
|-----------------------|------------|--------|--------|--------|------------|--------|--------|--------|------------|--------|--------|--------|------------|--------|--------|--------|
| Pedestrian trajectory | W wind | N wind | S wind | E wind | W wind | N wind | S wind | E wind | W wind | N wind | S wind | E wind | W wind | N wind | S wind | E wind |
| 1 | 1.68 | 1.68 | 1.70 | 1.72 | 1.68 | 1.67 | 1.67 | 1.68 | 1.67 | 1.67 | 1.67 | 1.68 | 1.67 | 1.67 | 1.68 | 1.67 |
| 2 | 1.69 | 1.68 | 1.71 | 1.72 | 1.68 | 1.67 | 1.67 | 1.69 | 1.68 | 1.67 | 1.67 | 1.68 | 1.68 | 1.68 | 1.69 | 1.68 |
| 3 | 1.74 | 1.73 | 1.76 | 1.77 | 1.72 | 1.70 | 1.73 | 1.74 | 1.72 | 1.70 | 1.72 | 1.74 | 1.73 | 1.73 | 1.73 | 1.73 |
| 4 | 1.74 | 1.73 | 1.76 | 1.77 | 1.71 | 1.70 | 1.72 | 1.74 | 1.71 | 1.70 | 1.74 | 1.74 | 1.74 | 1.74 | 1.73 | 1.73 |

worst than trajectories 1 and 2. That is related to the fact that trajectories 3 and 4 correspond to crossing the street in an area where PM_{10} concentration is higher and also due to fact that pedestrians need to spend more time (10 s more) in the street in these trajectories.

11 CONCLUSIONS

With the objective of studying the influence of building disposition and pedestrian trajectories in short-term human exposure to PM on a particular street in Portugal, an integrated system was developed. The integrated system considers a fully developed automatic system for the analysis of traffic profiles, a Gaussian model for the determination of traffic emissions (ADMS-Urban) and a CFD model (ANSYS Fluent) to simulate the dispersion of pollutants in the street canyon.

Four different configurations for the street, considering various building dimensions and gaps between buildings were simulated. Results show that the street configuration and building geometry have important influence on the results for PM_{10} concentration in the street.

Results also show that PM_{10} concentration is dependent on the predominant wind direction. The results for PM_{10} mean concentration at 1.5-m high for west wind and east wind directions show that the lower concentrations levels are obtained with configuration D (no gaps between buildings but same volume) because this geometry promotes the dispersion of pollutants as the wind is oriented with buildings, avoiding the formation of horizontal vortices in the building corners that promote the trapping of pollutants at pedestrian level. These results are in agreement with Refs [13–15].

For north wind and south wind directions (cross-canyon), configuration B is the one that results in lower concentrations. Gaps between buildings promote wind circulation crossing the street, improving pollutant removal and concentration for cross-canyon wind direction [16,17]. For these wind directions, there are no visible improvements in having bigger gaps (6 m) between buildings instead of 4-m gaps.

For the obtained PM_{10} concentrations, the level of short-term personal exposure is dependent on the pedestrian trajectory considered in the street. The best short-term exposure values are obtained for Scenario C, but the results are very similar to the ones obtained with Scenarios B and D. The worst short-term exposure results are obtained for Scenario A under East wind conditions, for pedestrian trajectories 3 and 4.

It is also possible to conclude that pedestrian trajectories 3 and 4 (crossing the street in the centre of the street) results in higher values for short-term personal exposure than trajectories 1 and 2. This is due to the fact that trajectories 3 and 4 correspond to pedestrian crossing the street in an area where PM_{10} concentration is higher and also due to the fact that pedestrians need to spend more time in the street.

ACKNOWLEDGEMENTS

The authors acknowledge Comissão de Coordenação e Desenvolvimento Regional de Lisboa e Vale do Tejo (CCDR-LVT) and Instituto de Meteorologia (IM) for the information provided.

REFERENCES

- [1] Martins, A., Cerqueira M., Ferreira F., Borrego C. & Amorim J.H., Lisbon air quality: evaluating traffic hot-spots. *International Journal Environment and Pollution*, **39**(374), pp. 306–320, 2009.
- [2] Amorim, J.H., Lopes, M., Borrego, C., Tavares, R. & Miranda, A.I., Air quality modelling as a tool for sustainable urban traffic management. Proceeding from *18th International Conference on Modelling, Monitoring And Management of Air Pollution*, ed. C.A. Brebbia & J.W.S Longhurst, WIT Transactions on Ecology and the Environment, 136, pp. 3–14, 2010.
- [3] Kumar, P., Ketzel M., Vardoulakis S., Pirjola L. & Britter R., Dynamics and dispersion modeling of nanoparticles from road traffic in the urban atmospheric environment – a review. *Journal of Aerosol Science*, **42**, pp. 580–603, 2011.
- [4] Garcia, J., Coelho, L., Gouveia C., Cerdeira, R., Louro, C., Ferreira, T. & Baptista M., Analyses of human exposure to urban air quality in a children population. *International Journal of Environment and Pollution*, **1/2/3**(40), pp. 94–108, 2010.
- [5] Domingos, J., M. Pinto. & Pontes, M., *Ocorrência média anual no território Português das classes de estabilidade atmosférica Pasquill-Guiford*. Técnico No. 460, XLII, pp. 27–42, 1980.
- [6] FLUENT, ANSYS Fluent 12.0, *Theory Guide*, ANSYS, Inc., 2009.
- [7] CERC, ADMS – Urban, *An Urban Air Quality Management System. User Guide – version 2.2*, CERC (Cambridge Environmental Research Consultants): Cambridge, UK, 2006.
- [8] Di Sabatino, S., Buccolieri, R., Pulvirenti, B. & Britter, R.E., Flow and pollutant dispersion in street canyons using fluent and adms-urban, *Environmental Modeling & Assessment*, **13**, pp. 369–381, 2008.
- [9] Awasthi S. & Chaudhry, K.K., Numerical simulation and wind tunnel studies of pollution dispersion in an isolated street Canyon. *International Journal of Environment and Waste Management*, **4**(1–2), pp. 243–255, 2009.
- [10] ANSYS, *Fluent Manual, Chapter 4. Turbulence*, ANSYS, Inc. January, 2009.
- [11] Garcia, J., Cerdeira, R., Tavares, N. & Coelho, L.M.R., Personal exposure to particle concentration in a busy street. *Air Pollution XX, WIT Transactions on Ecology and the Environment*, **157**, pp. 99–109, 2012. WIT Press. ISSN 1743-3541 (on-line) doi:10.2495/AIR120101.
- [12] Brown, M.J., Muller, C., Bush, B. & Stretz P., Exposure estimates using urban plume dispersion and traffic microsimulation models. *Proceedings of 10th Conference on Air Pollution Meteorology*, Phoenix, AZ, USA, Jan. 10–15, 1998.

- [13] Assimakopoulou, V.D., ApSimon, H.M. & Moussiopoulos, N., A numerical study of atmospheric pollutant dispersion in different two-dimensional street canyon configurations. *Atmospheric Environment*, **37**, pp. 4037–4049, 2003.
- [14] Chan, A.T., Au, W.T.W. & So, E.S.P., Strategic guidelines for street canyon geometry to achieve sustainable street air quality – part II: multiple canopies and canyons. *Atmospheric Environment*, **37**, pp. 2761–2772, 2003.
- [15] Wang, P., & Mu, H., Numerical simulation of pollutant flow and dispersion in different street layouts. *International Journal of Environmental Studies*, **67**, pp. 155–167, 2010.
- [16] Sagrado, A., Beeck, J., Rambaud, P. & Olivari, D., Numerical and experimental modelling of pollutant dispersion inside a street canyon. *Journal of Wind Engineering and Industrial Aerodynamics*, **90**, pp. 321–339, 2002.
- [17] Nikolova, I., Janssen, S., Vos, P., Vrancken K., Mishra, V. & Berghmans, P., Dispersion modelling of traffic induced ultrafine particles in a street canyon in Antwerp, Belgium and comparison with observations. *Science of the Total Environment*, **412**, pp. 336–243, 2011.